COMPACT ELECTRON GUN DESIGN FOR ULTRAFAST ELECTRON DIFFRACTION

Jasper J. Dargan
Old Dominion University, jdarg001@odu.edu

With

Advisor, Professor Hani Eslayed-Ali, Old Dominion University

Within this paper the construction of a compact pulsed electron gun for ultrafast electron diffraction is reported. This design utilized AutoCAD modeling and SIMION electron optic simulation. The electron gun consists of a sapphire (Al_2O_3) substrate (10 mm) in diameter with a 20 nm coated layer of silver for a laser-activated photocathode. The electron pulses are emitted by frequency-tripled femtosecond laser beam pulses that hit the thin film and then are accelerated by an electric field between the photocathode and a grounded anode. The electron beam is then collimated by a magnetic lens. Currently, beam profile characteristics are being configured and tested, however, completion of the gun is established and is emitting reasonable results at 35kv.

I. Introduction

Ultrafast Electron Diffraction (UED) allows in depth analysis of the crystal lattice structures of materials at the nanoparticle level. UED, like X-Ray diffraction, utilizes high energy electrons that pass-through objects to reveal their internal lattice structures. Generating these high energy electrons can be done by using an electron gun that is designed to take a laser pulse, up to the femtosecond level, and hit it against a photocathode that then releases the high energy electrons. These electrons are then focused by a magnetic field to allow more accurate precision when interacting with the material. After interaction, the electrons scatter and generate diffraction patterns. This procedure is exemplified in most reflection high-energy electron diffraction (RHEED) and transmission electron diffraction (TED) experimental setups.

The fundamental usage of this approach is to take advantage of the electron's sensitivity to nuclei. X-Rays do not interact with nuclei and therefore in conjunction both diffraction patterns can make a more complete picture of the molecular structure and even can construct "molecular movies", which show how the material changes over even 10 billionths of a second in thermal expansion.

Furthermore, electron guns have various usage within the scientific community. They are used in electron spectroscopy, electron laser beam machining, and electron microscopes for example. The electron gun can be considered as a lens that focuses the electrons onto a specimen. Electron beams can be emitted in various forms and can either be focused by electrostatic lenses or bent by magnetic lenses. The characteristics of an electron gun typically depend on its intended utility. For electron optical work, a fine beam of electrons is required and are usually emitted from a sharp tip. For electron beam machining, high-energy coherent photons are required. Since electron guns have such various demands, it is more appropriate to customize each electron gun for its intended usage.

II. Electron Propulsion and Optics

The theory behind electron gun design can be placed into two categories. The emission of electrons, and the flight path and characteristics of the electrons. For my design, I utilize basic photoemission techniques and a magnetic lens setup. The electron gun is activated by photoemission, this occurs with the aid of a femtosecond laser. Therefore, the photoelectric effect, Eq. (1) is essential, it describes the excitation and emission of electrons from metal surfaces when struck by light. For the sapphire substrate coated with silver to work I will need to utilize its low energy function to extract electrons.

$$Ekin = hw - \varphi \tag{1}$$

Where: h is Planck's constant, w, is the frequency of the incident photon and φ, is the work function of the metal. One technique to apply the photoelectric effect to electron gun design is to utilize a photocathode, essentially a metal attached to a substrate that will take the position of emitting electrons from within the gun after being activated by the laser pulse. The principle for this approach is to use a material that is inert, such as Au, or Ag, and house it on a substrate with a high transmissivity for UV light, high

thermal conductivity and vacuum capability such as sapphire.
The Lorentz Force Law, Eq. (2) will attribute to describing the amount of force or kinetic energy a point charge will experience, in this case the electron pulse packets, within an electric, magnetic or combination of electric and magnetic fields.

$$F = q\,(E + v \times B) \qquad (2)$$

Where: F is the Force present upon the electron, q is the charge of the particle, E is the electric field present, V is the velocity of the electron, B is the magnetic field present. Magnetic lenses utilize a non-uniform magnetic field with axial symmetry to focus electrons with a magnetic force. The force of the magnetic field is perpendicular to the magnetic field and the velocity of the electrons, this is shown in the Biot-Savart Law, Eq. (3)

$$B=(\mu_o 4\pi) \int IdI \times r|r|3 \qquad (3)$$

Where: B is the magnetic field, μ_o is the magnetic constant of the wire, I is the current passing through the wire, and r is the displacement vector of the wire. When an electron interacts at some point through a magnetic lens, it experiences all different forms of the magnetic field force. This produces a spiraling effect and correction; thus, producing a focusing action. That focusing power is dependent on the strength of the magnetic field and the characteristics of the particles that pass through the lens.
These principles are utilized within the following electron gun design.

III. Design

My design consists of a three-part triode electron gun. The components are a photocathode, pinhole/grid and anode Fig. 1.

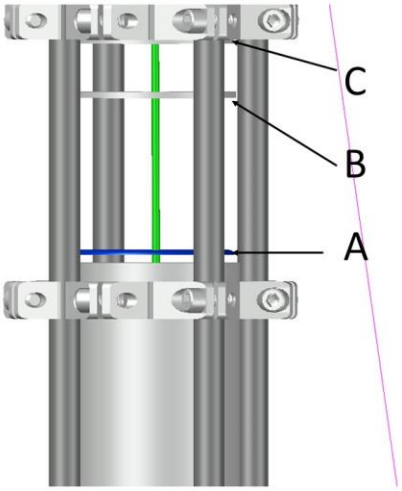

Fig. 1 AutoCAD model of triode “not drawn to scale”. (a) sapphire (Al_2O_3 10 mm diameter with silver 20 nm thin film coating. (b) 200-micron pin hole. (c) grounded anode.

The cathode consists of a sapphire (Al_2O_3) substrate (10 mm) in diameter with a 20 nm coated layer of silver. This will facilitate the electron creation, excitation and mark the exact zero point of travel for the electron to interact with the material. This is important to note because the distance from cathode to material will determine the overall effectiveness of the electron gun.

The cathode will be housed within an aluminum cylinder and connected to the high voltage source via a screw taping and wire. This will bring the overall cathode to a negative voltage designated by the high voltage feedthrough and facilitate the negative terminal of the electric field. The anode consists of a pinhole aluminum cylinder and mesh all housed within an aluminum cylinder. The pinhole is 200-microns ID. The mesh is an ultrathin grid. This mesh is adequate due to it not creating any interference under TEM experiments. The aluminum cylinder is also tapped and grounded to ground the entire anode system and complete the electric field for electron propulsion. Furthermore, there will be an added extension to the gun Fig. 2; a magnetic solenoid will be placed around the anode to utilize the capabilities of a magnetic focusing lens.

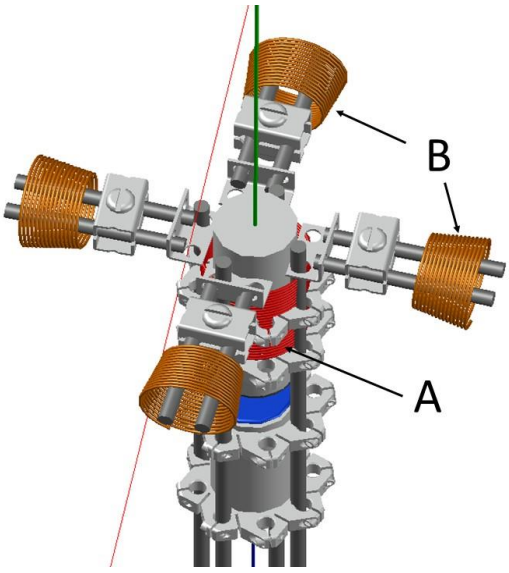

Fig. 2 AutoCAD model of magnetic focusing and deflection system, “not drawn to scale”. (a) magnetic solenoid wrapped around anode for immediate impact upon electrons entering the pinhole. (b) magnetic deflection in both x and y directions for centering of electrons.

I developed a magnetic coil system inside of the vacuum chamber that would allow the magnetic field focusing and reflection to take place as close as possible from the

emittance of electrons from the anode. The paradigm of the magnetic lens and reflection coils is in the order of lens and then reflection coils. The magnetic lens is wrapped around the aluminum housing for the anode thus the electrons experience the magnetic lens as soon as they transverse through the electric field. From here the magnetic deflection coils area attached to stainless-steel brackets and screw clamps and generate the magnetic field in both the X and Y directions. Once the electrons experience the magnetic reflection coils, they will interact with the test material with the minimum amount of distance available so that there is limited space charge effect.

IV. SIMION Simulation

SIMION is a very powerful tool that computes the complex electric, and magnetic field potentials and then properly conveys the influence it has upon an electron. It has a great capability to simulate the effectiveness of electron guns. The purpose of using SIMION will be to behave as an ion optics workbench and model then simulate an electron gun of my design.

To begin the modeling process, a configuration of the cubic grid dimensional "sandbox" where the simulation will virtually take place must be defined. This is created by generating potential arrays (PA), grid units that consists of grid points, and cells and replicate real space. PA's define the geometry of the electrodes/magnetic poles I design. They also express the potentials between electrodes and poles. The For my simulation, I created a 300x – 300y – 1z cylindrical potential array area. This gave me 300 grid units in both the x and y direction, each grid unit was the equivalent to 1mm in real space, to create my electron gun design. From this point I was able to replicate my physical design into virtual space Fig. 4-6.

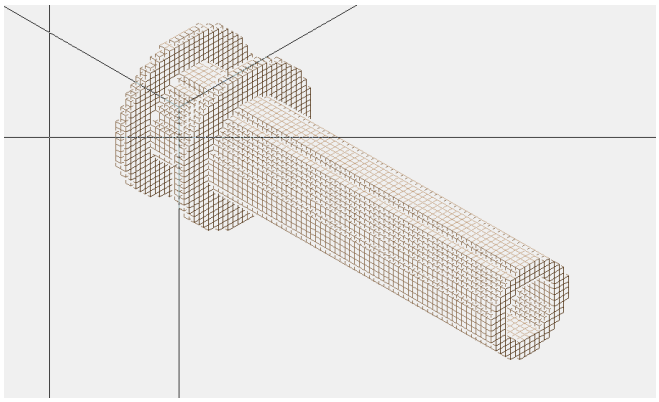

Fig. 3 SIMION modeling software representation of photocathode and anode pair in 3d space "Top left view"

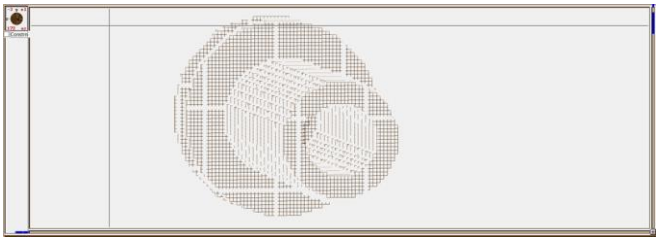

Fig. 4 SIMION modeling software representation of photocathode and anode pair in 3d space "Front facing view"

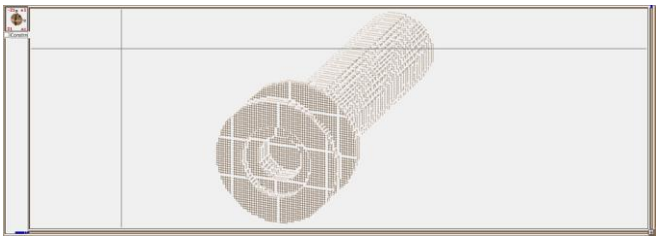

Fig. 5 SIMION modeling software representation of photocathode and anode pair in 3d space "Back facing view"

For my design simulation, I have set the two electrodes apart by 10 mm and the potentials as -60kv and 0v, see Fig. 7-8 for the photocathode and anode respectively. Regarding the solenoid magnetic potential, I have it set 350 Gauss**.**

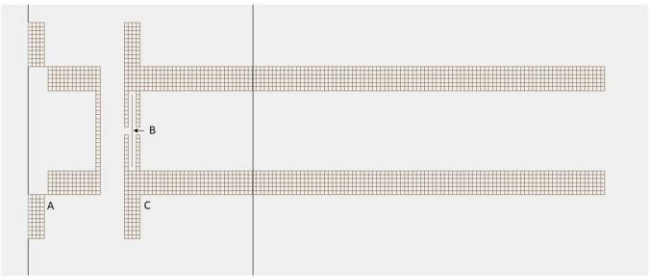

Fig. 6 2D representation of triode electron gun design, (A) Photocathode, (B) Pinhole/Grid, (C) Anode

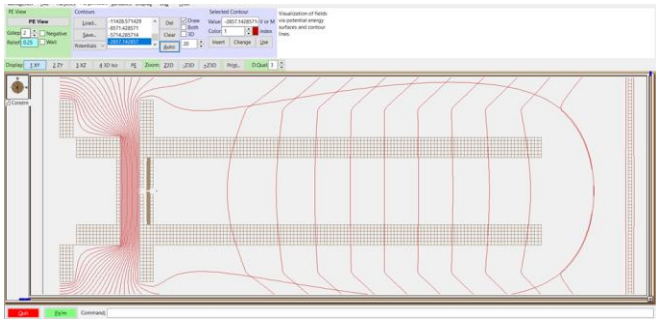

Fig. 7 2D representation of equipotential ray distribution at 60kv between photocathode and anode at 10 mm and equipotential ray distribution at 350 Gauss between both poles

For my design model, I had the electrons generate at the surface of the photocathode at 0 kinetic, energy with a 3D gaussian source distribution Fig. 8. This was to simulate the process of photoemission due to the femtosecond laser pulses hitting the photocathode. Once emitted, I set the parameters of the electrons to be grouped, thus they would experience space charge and coulombic repulsion forces.

This setup would allow me to get a more realist flight path of the electrons. The final parameter I set was the packet size of electrons; I decided to run 6,000 electrons per simulation two different times. Once, under the effect of the electric field only and again with both the electric field and magnetic field potentials.

For my analysis of the simulation I have decided to record eight parameters: Time of flight (TOF), x, t, and z coordinate positions once trajectory ends, kinetic energy (KE) KE error, and hit count, or how many electrons managed to complete

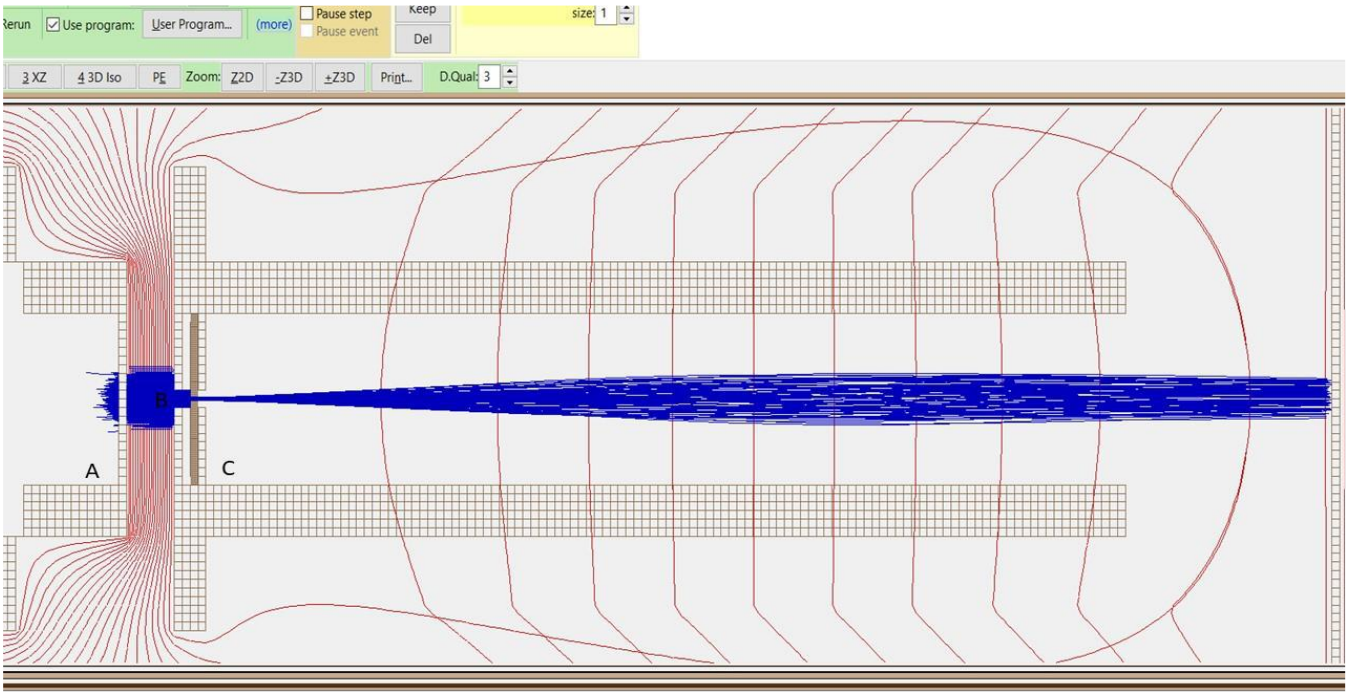

Fig. 8 2D triode configuration with simulation start. Simulates the photoemission of electrons, “in blue” from the (A) photocathode, entering the (C) anode, passing through (B) mesh grid and pinhole and traveling through the anode tube (Electric Field and Magnetic Field)

their trajectory and hit the intended target, see Table. 1.

These parameters are great indicators on the emittance and coherence of the electron beam. To put simply, the faster the TOF and KE the better the emittance. The KE error will allow me to see if there is any loss of energy when the electrons are emitted. Furthermore, mapping the x, y, z coordinates of the electrons that hit the target can showcase the coherence of the beam, while also visualizing the effects of coulombic forces and space charge effects on the beam.

	Electric Field	Electric & Magnetic Field
AVG Time of Flight (TOF)	9.59E-04s	9.50E-04s
AVG Kinetic Energy (KE)	59870J	59867J
AVG Kinetic Energy Error	2.1%	2.0%
Hit Count	798	794
Electron Loss	20.2%	20.6%

Table. 1 This table showcases the recorded data of the emitted electrons, both with the effects of the electric field separately and magnetic field congruently.

Regarding the coherence of the beam, I have looked at the y and z axis recorded data to see the spread of the electrons as they hit the material Fig. 9.

Fig. 9 (below) x and y coordinate mapping of electrons that hit material showcasing the beam coherence of the simulation. (With electric and magnetic field)

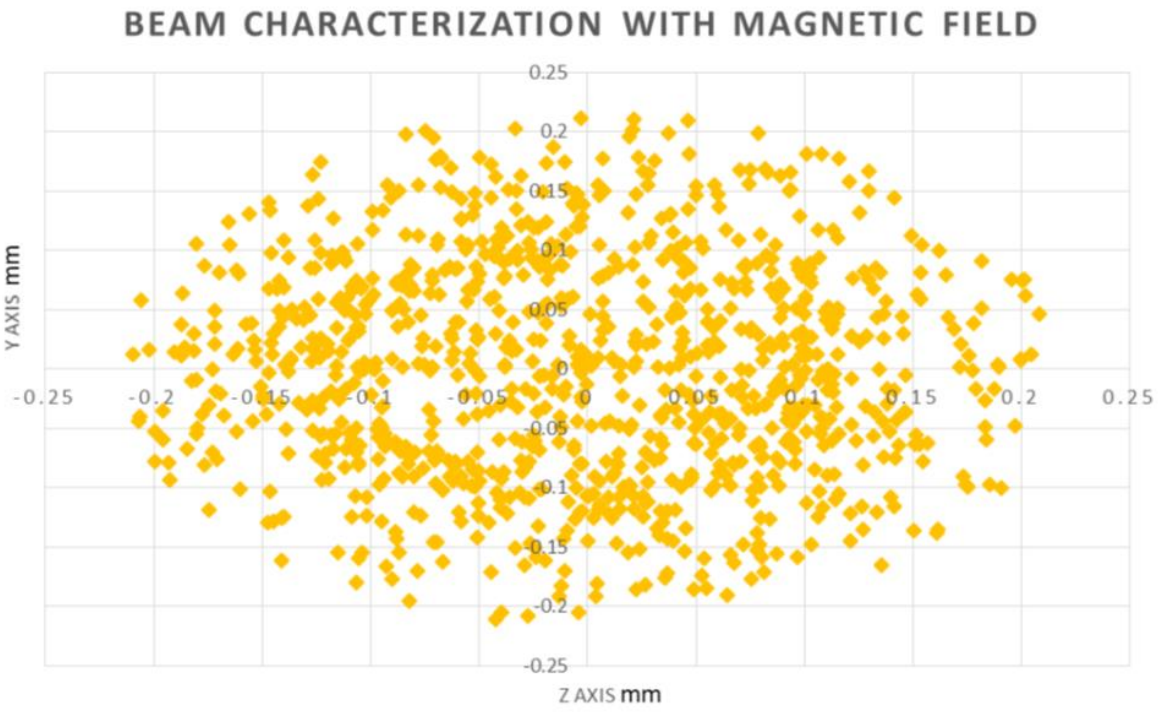

V. Manufacturing and Testing

The complete design has been established and is incorporated within a vacuum chamber for electron beam characterization testing Fig. 10.

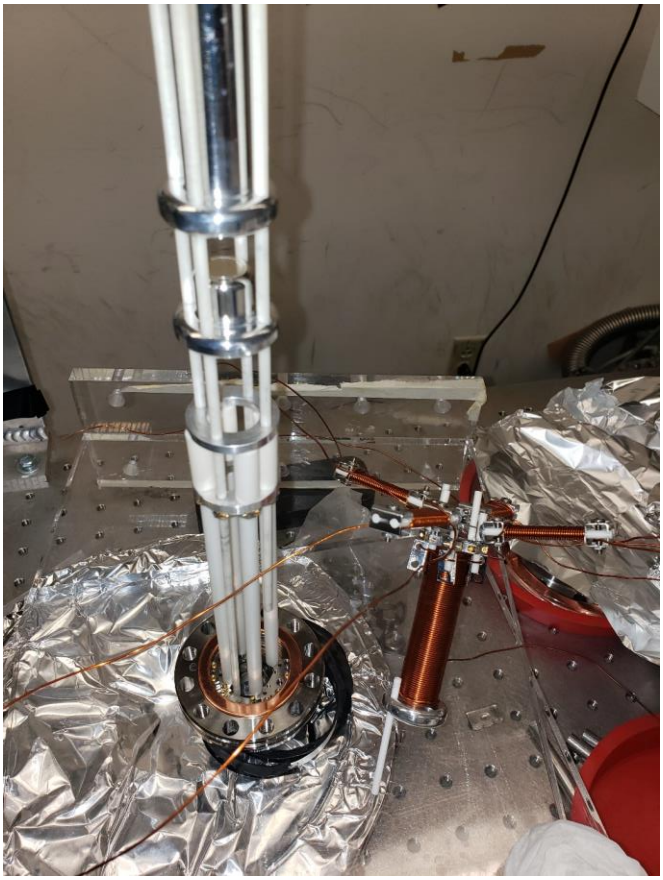

Fig. 10 Picture taken of complete unassembled electron gun. (left) Assembled photocathode and anode configuration. (right) Assembled magnetic focusing and deflection plates. (bottom) Complete assembled electron gun fitted within vacuum chamber and attached to 8" flange shown with Helium-Neon laser emitting through anode exit aperture.

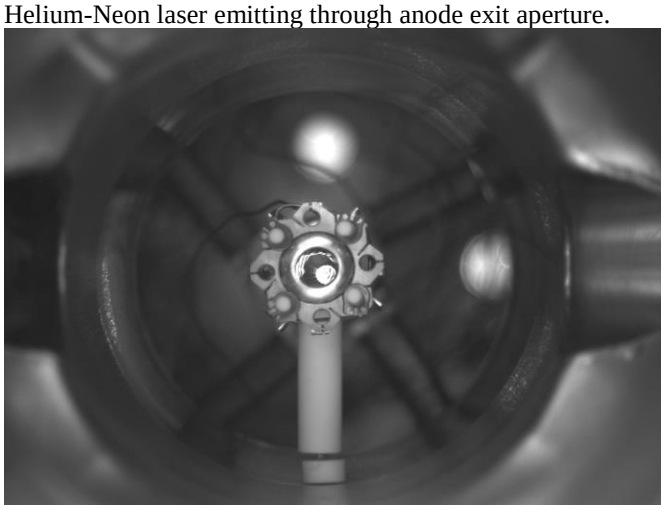

The vacuum chamber has an external magnetic field for added focusing and contains power feedthroughs for the internal magnets.

The distance between photocathode and anode is between 8mm-10mm. Testing has been conducted under 35kv and electron beam imaging has been captured upon a phosphorus screen using a camera Fig. 11.

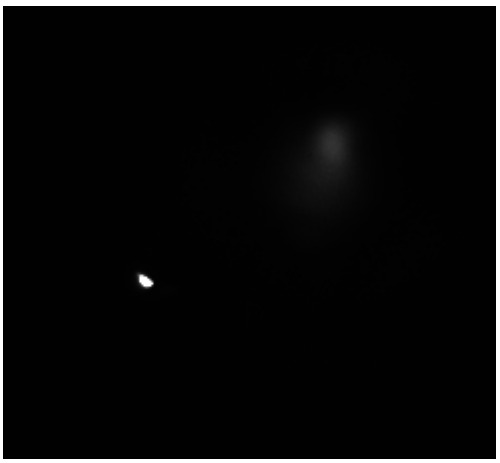

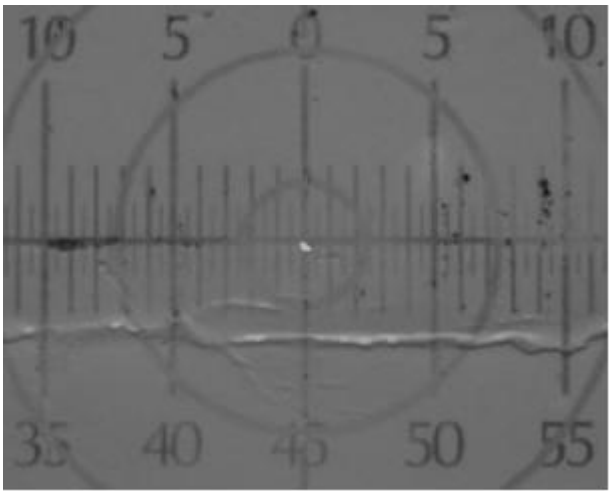

Fig. 11 (top) Focused electron beam spot displayed upon phopshor screen in dark room. Slight abberition within the center created by femtosecond laser. (bottom) electron beam spot displayed upon mm scale.

Chamber conditions were under vacuum pressures at 10^{-7} Torr levels. At these levels, voltage was slowly applied to the photocathode while also being exposed to the femtosecond laser. At this point, any electrical sparks that were observed, either physically by sight or hearing and digitally by observing the change in pressure, was recorded down for future reference. The maximum voltage that has been stably recorded has been at 35kv. Current beam spot size is being determined but appears to be under 1 mm.

VI. Conclusion

The creation of the electron gun has been successfully fulfilled and is now going through physical testing for verification and comparison to the digital simulation. The usage of a 20 nm Ag thin film photocathode in conjunction with a femtosecond UV laser for photoemission has been successful and can work at 35kv under stable conditions. Further steps are to troubleshoot any sparking issues that occur so that a new level of applied voltage can be attained closer to 60kv. Furthermore, the implantation of a faraday cup within the chamber will be used for the collimation of the electron beam to gather the current density of the beam. Then, the application of a material sample will be used to create a diffraction pattern with which the spatial resolution of the electron gun can be determined from the transfer width of the patterns. These added data elements will be able to define the utility of the electron gun more accurately.

Acknowledgements

This paper and all the work it encompasses would not have been completed without the aid of my advisor professor Hani Eslayed-Ali, all of our team members past and present and of course the Virginia Space Grant Consortium partnered with NASA for giving me financial support.

H. E. Elsayed-Ali and G. A. Mourou, Picosecond reflection high-energy electron diffraction, Appl. Phys. Lett. 52, 103-104 (1988).

2. H. E. Elsayed-Ali and J. W. Herman, Ultrahigh vacuum picosecond laser-driven electron diffraction system, Rev. Sci. Instrum. 61, 1636-1647 (1990).

3. H. E. Elsayed-Ali and J. W. Herman, Picosecond time-resolved lattice surface temperature probe, Appl. Phys. Lett. 57, 1508-1510 (1990).

4. H. E. Elsayed-Ali, System for surface temperature measurement with picosecond time resolution, U.S. Patent No. 5,010,250, April 23, 1991.

5. M. Aeschlimann, E. Hull, C. A. Schmuttenmaer, J. Cao, L. G. Jahn, Y. Gao, H. E. Elsayed-Ali, D. A. Mantell, and M. Scheinfein, A picosecond electron gun for surface analysis, Rev. Sci. Instrum. 66, 1000-1009 (1995).

6. H. E. Elsayed-Ali, Time-resolved high-energy electron diffraction, in 23rd International Congress on High-Speed Photography and Photonics, edited by V. P. Degtyareva, M. A. Monastyrski, M. Y. Schelev, and A. V. Smirnov, SPIE Proceedings, Vol. 3516, 607-615, P. N. Lebedev Physical Institute, Moscow, Russia, 20-25 September, 1998.

7. B.-L. Qian and H. E. Elsayed-Ali, A new compensating element for a femtosecond photoelectron gun, Rev. Sci. Instrum. 72, 3507-3513 (2001).

8. B.-L. Qian and H. E. Elsayed-Ali, Electron pulse broadening due to space charge effects in a photoelectron gun for electron diffraction and streak camera systems, J. Appl. Phys. 91, 462-468 (2002).

9. B.-L. Qian and H. E. Elsayed-Ali, Acceleration element for femtosecond electron pulse compression, Phys. Rev. E 65, 046502 (2002).

10. B.-L. Qian and H. E. Elsayed-Ali, Comment on ''Ultrafast electron optics: Propagation dynamics of femtosecond electron packets, J. Appl. Phys. 92, 1643 (2002), J. Appl. Phys. 94, 803-806 (2003).

11. T. Frigge, B. Hafke, V. Tinnemann, T. Witte, and M. Horn-von Hoegen, Spot profile analysis and lifetime mapping in ultrafast electron diffraction: Lattice excitation of self-organized Ge nanostructures on Si(001), Structural Dynamics 2, 035101 (2015).

12. X. Wang, S. Nie, H. Park, J. Li, R. Clinite, R. Li, X. Wang, and J. Cao, Measurement of femtosecond electron pulse length and the temporal broadening due to space charge, Rev. Sci. Instrum. 80, 013902 (2009).

13. M. Harb, H. Enquist, A. Jurgilaitis, F. T. Tuyakova, A. N. Obraztsov, and J. Larsson, Phonon-phonon interactions in photoexcited graphite studied by ultrafast electron diffraction, Phys. Rev. B 93, 104104 (2016).

14. B. J. Siwick, A. A. Green, C. T. Hebeisen, and R. J. D. Miller, Characterization of ultrashort electron pulses by electron-laser pulse cross correlation, Opt. Lett. 30, 1057-1059 (2005).

15. R. C. Dudek and P. M. Weber, Ultrafast diffraction imaging of the electrocyclic ring-opening reaction of 1,3-cyclohexadine, J. Phys. Chem. A 105, 4167-4170 (2001).

16. A. Hanisch, B. Krenzer, T. Pelka, S. Mollenbeck, and M. Horn-von Hoegen, Thermal response of epitaxial thin Bi films on Si(001) upon femtosecond laser excitation studied by ultrafast electron diffraction, Phys. Rev. B 77, 125410 (2008).

17. G. H. Kassier, K. Haupt, N. Erasmus, E. G. Rohwer, and H. Schwoerer, Achromatic reflection compressor design for bright pulses in femtosecond electron diffraction, J. Appl. Phys. 105, 113111 (2009).

18. A. H. Zewail, Diffraction, crystallography, and microscopy beyond three dimensions: Structural dynamics in space and time, Phil. Trans. R. Soc. A 363, 315-329 (2005).

19. A. Gahlmann, S. T. Park, and A. H. Zewail, Ultrashort electron pulses for diffraction, crystallography and microscopy: Theoretical and experimental resolutions, Phys. Chem. 10, 2894-2909 (2008).

20. L. Waldecker, R. Bertoni, and R. Ernstorfer, Compact femtosecond electron diffractometer with 100 keV electron Bunches approaching the single-electron pulse duration limit, J. Appl. Phys. 117, 044903 (2015).

21. M. Abdel-Fattah, A. Bugayev, and H. E. Elsayed-Ali, Lattice dynamics of femtosecond laser-excited antimony, Physica B: Physics of Condensed Matter 492, 65-69 (2016).

22. Greenberger, Daniel M., et al. Compendium of Quantum Physics: Concepts, Experiments, History and Philosophy. Springer, 2009.

23. Ischenko, A. A., et al. "A Stroboscopical Gas-Electron Diffraction Method for the Investigation of Short-Lived Molecular Species." Applied Physics B Photophysics and

Laser Chemistry, vol. 32, no. 3, 1983, pp. 161–163., doi:10.1007/bf00688823.
24. "Advances in Imaging and Electron Physics." Advances in Imaging and Electron Physics, 2010, doi:10.1016/c2009-0-62328-x.
25. Klimkowski, V. J., et al. "Molecular Orbital Constrained Electron Diffraction Studies. 4. Conformational Analysis of the Methyl Ester of Glycine." Journal of the American Chemical Society, vol. 104, no. 6, 1982, pp. 1476–1480., doi:10.1021/ja00370a004
26. "Advances in Imaging and Electron Physics." Advances in Imaging and Electron Physics, 2010, doi:10.1016/c2009-0-62328-x.
27. (Institut Fuer Angewandte Physik Der Universi, Kasper Erwin. Principles of Electron Optics, Volume 1 - Basic Geometrical Optics. Vol. 1, Elsevier Science & Technology, 2017.
28. Egerton, R. F. Physical Principles of Electron Microscopy: an Introduction to TEM, SEM, and AEM. Springer Science Business Media, 2007.
29. Egerton, R. F. Physical Principles of Electron Microscopy: an Introduction to TEM, SEM and AEM. Springer, 2016.
30. KHARAGPUR IIT. "Electron Beam and Laser Beam Machining." Non conventional Machining. nptel.ac.in/courses/112105127/40.
30. Greenberger, Daniel M., et al. Compendium of Quantum Physics: Concepts, Experiments, History and Philosophy. Springer, 2009.
31. Grivet, Pierre. Electron Optics P. Grivet with with Collaboration of M.Y. Bernard 2d English Ed., Rev. Afresh by A. Septier. 2nd ed., Pergamon Press, 1972.
32. Klimkowski, V. J., et al. "Molecular Orbital Constrained Electron Diffraction Studies. 4. Conformational Analysis of the Methyl Ester of Glycine." Journal of the American Chemical Society, vol. 104, no. 6, 1982, pp. 1476–1480., doi:10.1021/ja00370a004.
33. Rose, Harald H. Geometrical Charged-Particle Optics. Springer, 2009.
34. Spicer, W. E., A. Herrera-Gomez, "Modern theory and applications of photocathodes," Proc. SPIE Int. Soc. Opt. Eng: Photodetectors and Power Meters 2022, 18 (1993).
35. Wang, X. J., et al, "Experimental observation of high-brightness microbunching in a photocathode rf electron gun," Phys. Rev. E 54, R3121 (1996).
36. "Chapter 2. SIMION Basics (SIMION® 8.0 User Manual)." Definition: Child's Law, simion.com/manual/chap2.html.
37. "Electron Optics of Point Cathode Electron Gun." Journal of Electron Microscopy, 1983, doi:10.1093/oxfordjournals.jmicro.a050409.
38. "Importing a Solenoid Magnetic Field into SIMION by Multiple Methods." Definition: Child's Law, simion.com/docs/solenoid.html.
39. Ives, Lawrence, et al. "Computer Optimization of Electron Guns Using Beam Optics Analysis." 2007 IEEE International Vacuum Electronics Conference, 2007, doi:10.1109/ivelec.2007.4283361.
40. Kozhevnikov, Vasily Yu., et al. "Modeling of Space Charge Effects in Intense Electron Beams: Kinetic Equation Method Versus PIC Method." IEEE Transactions on Plasma Science, vol. 45, no. 10, 2017, pp. 2762–2766., doi:10.1109/tps.2017.2726501.
41. Maloff, I.g., and D.w. Epstein. "Theory of Electron Gun." Proceedings of the IRE, vol. 22, no. 12, 1934, pp. 1386–1411., doi:10.1109/jrproc.1934.227204.
42. "SIMION® Version 8.1." Definition: Child's Law, simion.com/.